I.A.U
Karaj branch

Journal of
A p p l ied
C hemical
R esearch
jacr.kiau.ac.ir

Journal of Applied Chemical Research, 15, 3, 58-75(2021)

Development of a Pre-concentration Method for Nickel in Chocolate Samples using Magnetic Dispersive Solid- phase Extraction Followed by Flame Atomic Absorption Spectrometry

Vahid Mortazavi Nik[1], Elaheh Konoz[1,*], Alireza Feizbakhsh[1],Amir Abdullah Mehrdad Sharif[2]

[1]Department of Chemistry,Central Tehran Branch, Islamic Azad University, Tehran, Iran

[2]Department of Chemistry, Islamic Azad University, North Tehran Branch, Tehran, Iran

(Received 04Nov. 2020; Final revised received 12Feb. 2021)

Abstract

In this study, magnetic dispersive solid-phase extraction (MDSPE) combined flame atomicabsorption spectrometry (FAAS) was used as a new method for the analysis of nickel preconcentration in chocolate samples. A suitable mixture of magnetic adsorbent 1(2,3-dihydroxypropyl)-1,4diazabicyclo[2.2.2] octanylium [DABCO-PDA] and chloro-functionalized Fe_3O_4 nanoparticles (NPs) with chelating agent dimethylglyoxime (DMG) was added into an aqueous solution. Adsorption behaviors of Ni (II) ion on Fe-[DABCO-PDA] NPs were studied. Finally, the main parameters affecting the extraction and determination of the analysis were investigated in detail.According to the findings, the analyte was quantitatively holed on Fe-[DABCO-PDA] NPs in pH 8, eluted totally with 3 ml of ethanol HNO_3 2% (v/v), and adsorbed about 50 mg. Under the optimal experimental conditions, the detection limit (LOD) was 0.18 µg Kg^{-1}, with a standard deviation of1.8-4% (n=5). The linear working range of the calibration curve was 1-250 µg Lit^{-1} and the recovery values ranged from 92 to 97% for all samples. The proposed method was fast, simple, effective and high tolerability to the presence of the ions. Moreover, high sensitivity, better recovery, and the use of environmentally friendly solvents are the other advantages of this technique.

Keywords: Dispersive Micro solid-phase extraction, Flame atomic absorption spectrometry, Nickel, Fe-[DABCO-PDA] NPs.

[*] ***Corresponding author:*** Elheh *Konoz*,*Department of Chemistry, Central Tehran Branch, Islamic Azad University, Tehran, Iran*. *Email: Konozelaheh@gmail.com*.

Introduction

Today, rapid urbanization and industrial development has been accompanied by an increase in metal pollution. Most of the metal ions are highly toxic and become degraded hardly. These elements, like nickel, have long half-lives and accumulate easily in living organisms[1,2]. This metal presents in jewelry, cosmetics,[3] water,[4] food,[5] and biological fluids[6]. The nickel level in plain chocolate is within the range of 0.05-10.3 mg kg^{-1}, which makes it an important source of nickel[7,8]. So, it is important to measure it because of the children's interest in chocolate. Nickel is measured through separation and pre-concentration methods [9] such as liquid phase extraction, solid-phase extraction (SPE), coprecipitation, and cloud point extraction (CPE)connection with different detection techniques[10–14]. Divers instrumental approaches were widespread and joined for determining the metal ions in samples, inclusive atomic absorption spectrometry (AAS), atomic fluorescence spectrometry (AFS), X-ray spectrometry, inductively coupled plasma atomic emission spectrometry (ICP-OES), neutron activation analysis, and inductively coupled plasma mass spectrometry (ICP-MS)[15–20]. The sample analysis by these methods is normally limited because of the extremely low concentration of analytes and matrix effects. Thus, pretreatment approaches of the sample are generally needed before the analysis[21]. Dispersive micro solid-phase extractions (DMSPE) with magnetic nanoparticles have been used as a new method for sample preparation[22–25]. Ionic liquids (ILs) as some organic salts are composed of various non-organic, organic anions and organic cations[26–28]. Thus, modification of magnetic nanoparticles with ILs can be joined to gather the benefit of the ILs and magnetic NPs, as well as enhancing the extraction capability for some analytes[29–33].

The present work for the first time presents a new magnetic adsorbent Fe_3O_4 modified with DABCO-IL in DMSPE for the separation and pre-concentration of nickel from aqueous samples. In this research, dimethylglyoxime (DMG) was used to increase selectivity and overcome the uptake of other ions. The benefits of this magnetic nano-adsorbent include its chemical stability, high adsorption capacity, less adsorbent dose, short extraction time, large surface area, rapid phase separation, high adsorption activity and low toxicity[34–40].The experimental parameters influencing DMSPE, including eluent parameters, pH, sample volume, adsorbent dose, contact time, and ligand concentration, were studied. Based on empirical findings, a new process coupling DMSPE, DABCO-IL, and FAAS was developed for determining trace nickel in chocolate samples with reasonable accuracy.

Experimental

Instrumentation

A Perkin Elmer flame atomic absorption spectrometer (pinAAcle 900T, USA) equipped with a nickel hollow cathode lamp at 232 nm was used for measuring the analytes. A pH meter (Metrohm, Switzerland) with a combined electrode was employed for controlling the pH of the solution. An ultrasonic bath (Bandelin, Germany) was utilized. A shaker (Heidolph, Germany) was used for mechanical stirring. Also, a rotary evaporator (Heidolph Hei-VAP, Germany) was applied. A microwave digestion device (Analytical Jena, Germany) was applied for the digestion of the solid sample. Finally, phase separation was done using a magnet.

Chemicals and Reagents

All the reagents employed in the current study were of analytical grade. The standard nickel solution was provided by dilution of a 1 mg L^{-1} stock standard solution of $Ni(NO_3)_2.6H_2O$ (Merck, Darmstadt, Germany) using ultrapure water (from a water purification system, Evoqua, Italy with electrical conductivity below 0.06µscm^{-1}), Iron (III) chloride hexahydrate, tetraethyl orthosilicate, Iron(II) chloride tetrahydrate, (3-chloropropyl)trimethoxysilane, DABCO,3-chloro-1,2-propanediol(Sigma-Aldrich, Germany), methanol, ethanol, acetonitrile.The adjustment of solution pH was per-formedusing 0.1M HCl or 0.1M NaOH solution as needed. All glasswares were cleaned by drenching in a 5% (v/v) nitric acid solution during one day. Then, it was washed with deionization water.

Synthesis of Fe-[DABCO-PDA] NPs

Synthesis of Fe_3O_4 NPs

The preparation steps of Fe_3O_4 NPs were explained in the previous study [41].The samples were prepared using a chemical co-precipitation method. The black Fe_3O_4NPs were gathered by a strong magnet and rinsed with ethanol and deionized water.

Synthesis of Fe- SiO_2Core-Shell

The SiO_2 layer was used to coat the surface in accordance with the modified Stöber method[42].Briefly, the prepared Fe_3O_4NPs were used as centers and dispersed in ethanol (220 ml), and then the mixture was delivered to a three-neck flask with a round-bottom. The mixture was stirred for 60 min and then 100 ml ammonia solution was added to it. After 1 h, 3 ml tetraethyl orthosilicate (TEOS) was added slowly to the mixture. The mix was mechanically stirred for 12 h to

complete the silica coating. The generated Fe-SiO_2 was separated and rinsed with ethanol and a50:50(v/v) deionized water.

Chloro-functionalization of Fe- SiO_2 NPs

The Fe_3O_4NPs cores were coated with the silica layer. Fe_3O_4NPs were produced based on chloro-functionalization[43]. Briefly, 2 g Fe-SiO_2 NPs were dissolved in 200 ml of toluene by mechanical stirring. While the mixture was strongly stirred, 2 ml of(3-chloropropyl) trimethoxy silane (CPTMS) was added slowly, and the reaction was continued at 60 °C for 18 h. Then, precipitates were collected by the magnet and washed with toluene.

DABCO based-IL Synthesis

DABCO-PDA was synthesized based on the method proposed in the previous study[44].DABCO (22.5 g) was put in a 250 ml round-bottom flask and was solved in ethanol (100 ml). Afterward,3-chloro-1, 2-propanediol (17 ml) was added to the mixture. Finally, the solution was refluxed for one day.

Synthesis of DABCO-based IL-functionalized Fe_3O_4NPs

The DABCO-based IL-functionalized Fe_3O_4NPs was obtained based on an approach previously reported. Briefly, 1 g of Fe-CPTMS NPs was dispersed in 200 ml ethanol by sonication. Then,4 g of [DABCO-PDA] was added to the mixture. The suspension was heatedto reflux with mechanical stirring for 1 day. Afterward, the magnetic particle Fe-[DABCO-PDA] NPs were separated by a magnet and washed with ethanol and deionized water .

Sample Preparation

To prepare samples (Chocolate 55%, Chocolate75%, Chocolate85%, and Chocolate Shoniz), 300mg was weighed and transferred into Teflon tubes of 100 ml. 6 ml HNO3 65% and 2ml H2O2 30% were added to each of them. The digestion tubes were sealed and placed in a microwave oven. Then, the samples were digested in the microwave oven. The operating conditions for microwave digestion are listed in Table1.

Table1. Operating parameters for microwave digestion.

Temperature program	Step	1	2
	T[C°]	145	190
	P[bar]	40	40
	Power[%]	70	90
	Time[min]	10	15

The solution was delivered into a volumetric balloon after cooling. The residue wasdissolved with 0.1 mol $L^{-1}HNO_3$ and suspended to a true volume and then kept at 4°C before application.

Results and discussion

Fe-[DABCO-PDA] NPs Characterization

XRD Analysis

XRD spectroscopy was used for the analysis of the crystalline structure in the prepared NPs (Figure 1a). The diffraction peaks observed at 2Θ=35.3°, 42.1°, 50.2°, 63.5°, 67.7°, and 73.8° are corresponded to (220), (311), (400), (422), (511), and (440) planes, respectively. These results suggest the presence of a magnetite phase with a cubic spinal as a highly crystalline structure[45].In addition, detecting no impurity peaks verifies that the synthesized Fe_3O_4NPs have a pure phase.Figure1a shows that diffraction peaks of Fe-[DABCO-PDA] were weaker and the crystallinity decreased in the IL-functionalized Fe_3O_4NPs.

The magnetic characteristics

The magnetic characteristics of the produced Fe_3O_4NPs, Fe-SiO_2, and Fe-[DABCO-PDA] were studied by VSM at room temperature. Figure1b illustrates the hysteresis loops related to superparamagnetic behavior for all the NPs. After extraction of a magnetic field, the magnetism of NPs was not kept[46].The saturation magnetization (MS) values of the non-coated Fe_3O_4NPs were estimated to be 60, 41, and 25 emu g^{-1} for Fe-SiO_2, Fe-[DABCO-PDA], and Fe_3O_4NPs, respectively, lower than that of the uncoated particles. These results show that the magnetization of Fe_3O_4NPs decreased extremely by increasing the SiO_2 and IL shell. The superparamagnetic feature of the synthesized magnetic NPs material is very important for its application such as magnetic solid-phase extraction[47,48].

Thermogravimetric Analysis

The thermal stability of the Fe_3O_4NPs, Fe-SiO_2, and Fe-[DABCO-PDA] was confirmed by TGA (Figure 1c). The TGA curves of all samples depict a three-step weight loss. The first weight loss of

2% in the 110-200°C was due to the elimination of physics sorbet water molecules available in the pores and on the external surface. The second step weight loss of 18% appeared in the temperature range of 200-600°C, which is due to the thermal decomposition of the organic functional groups on Fe_3O_4NPs surface. The third weight loss of about 2%, which occurred at temperatures above 600°C, is related to the self-compaction of the silanol groups.

FTIR Spectra

The FTIR spectra of Fe-SiO_2, Fe_3O_4, Fe-SiO_2-CPTMS, and Fe-[DABCO-PDA] NPs are shown in Figure1d. For the magnetic nano-particles (Figure 1da), the stretching vibration bands at 567 cm^{-1} are the generic IR absorbance induced by Fe-O vibration[49].There is a wide band at 3420 cm^{-1} and a narrow band at 1620 cm^{-1} that are attributed to adsorbed water or the hydroxyl bending on the surface of the sample. After coating the magnetite NPs with silica layer (Figure 1db), the wide high-intensity bond at 1072 cm^{-1} and 800 cm^{-1} are because of the Si-O-Si asymmetric stretching vibration and stretching vibration of Si-O-H. Among all these bands (Figure 1dc), SiO_2 was successfully coated on the surface of Fe_3O_4 NPs. For Fe_3O_4-CPTMS, two absorption peaks at 2850 and 2990 cm^{-1} are assigned to stretching vibration in the methylene groups.Moreover, asymmetric Si-CH_2-CH_2-$CH_2$and C-Cl stretching vibration observed at 1300 cm^{-1} and 780 cm^{-1} (Figure 1dd) because of the deposition of CPMTS onto the magnetic Fe-SiO_2 NPs. For the FTIR spectrum of the Fe_3O_4-[DABCO-PDA] NPs, two absorption peaks at 550 and 3450 cm^{-1} are because of the stretching vibration of Fe-O and-OH. Moreover, an absorption band at 1460 cm^{-1} is assigned to the stretching vibration of C-N^+-C group. These bonds suggest that the Fe_3O_4 NPs are functionalized successfully with [DABCO-PDA].

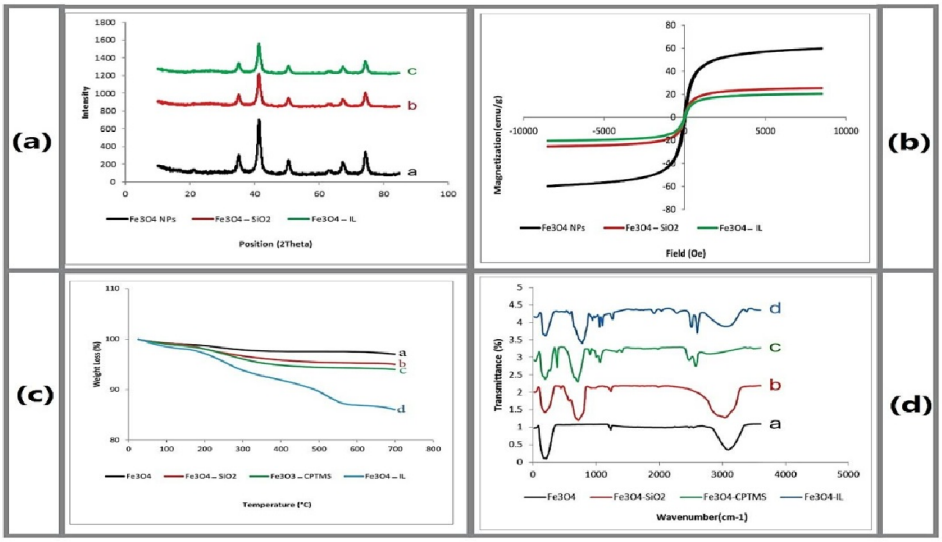

Figure 1. (a) XRD image, (b) Magnetization curves, (c) TGA curves, and (d) FT-IR spectra*EDX, FE-SEM, TEM Analysis.*

The elemental analysis of the composition was done using the EDX (Figure2a). This spectral model confirms the existence of strong peaks of oxygen, silicon, and iron, indicating that O, Fe, and Si are the main elements in the composition. In addition, small peaks related to the N and C are seen in these spectra. The EDX spectrum confirms that Fe_3O_4 core-shell NPs were functionalized successfully with [DABCO-PDA].

The morphological structure of the Fe_3O_4, Fe-SiO_2, chloro-functionalized Fe_3O_4, andFe-[DABCO-PDA] nanoparticles was studied by FE-SEM (Figure 2b). The results show that the Fe-[DABCO-PDA] nanomaterials have a spherical and homogenous structure. The mean diameter Fe_3O_4 NPs, Fe-SiO_2NPs, chloro-functionalized Fe_3O_4, and Fe-[DABCO-PDA] was nearly 12 nm, 16 nm, 27 nm, and 32 nm, respectively.

The TEM images of magnetic nanoparticles are shown in Figure2c. TEM technique was applied to provide a better understanding of the configuration of the magnetic NPs functionalized with IL. As can be seen, a magnetic/IL core-shell configuration was expanded. According to Figure 2c, a gray shell coated the dark core of Fe3O4. The porous structure of the compounds related to the products increases surface area and provides availability to the target molecules.

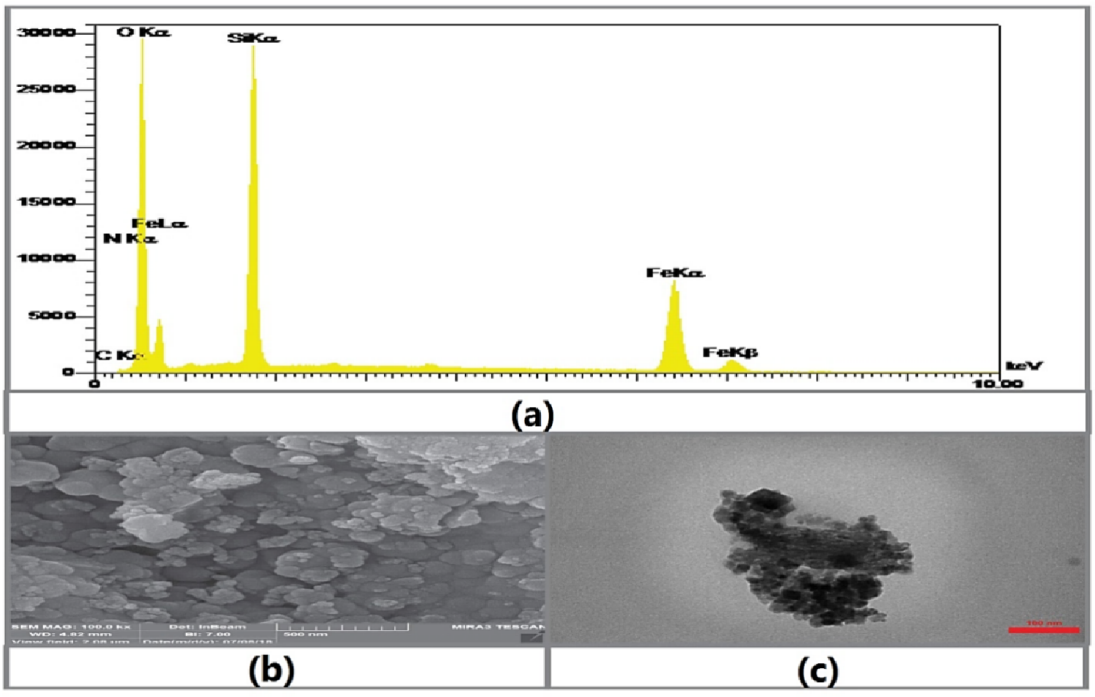

Figure 2. (a) EDX, (b) FE-SEM, and (c) TEM of Fe-[DABCO-PDA].

Effect of pH

The present form of analytes and sorbent surface charges were considerably influenced by the pH of a sample solution. This effect was tested in the range of 2 to 11 (Figure 3a). The results show that at

low pH, the extraction efficiency is low, which can be attributed to the competition between H^+ and Ni^{2+} in interaction with the ligand donor electron groups.At higher pHs, the concentration of H^+ to bind to the ligand decreases, thus the extraction efficiency was improved. Ni^{2+} is the only important oxidation state in the aqueous solution as $[Ni(H_2O)_2]^{2+}$. At pH>8, Ni^{2+} precipitates as $Ni(OH)_2$ because of the existence of hydroxide anions[50,51]. Therefore, pH 8 was chosen in this experiment.

Effect of adsorbent dose

The amount of adsorbent as another important parameter affects the metal cation inhabitation and pre-concentration. In the constant concentration of metal ions, the more amount of absorbent provided a larger surface and more sites to adsorb cation. At a low amount of the adsorbent, the surface is saturated with metal complexes remained in the solution. To bring the optimal level of sorbent needed for the quantitative readjustment of the analytes, various Fe-[DABCO-PDA] NPs were examined from 10 to100 mg per sample solution (25 ml). The results indicated that the quantitative readjustment (>90%) of the analytes might be achieved using the amount of Fe-[DABCO-PDA] NPs ranging from 50 to 100 mg. Thus, 50mg Fe-[DABCO-PDA] NPs were used in the following experiments (Figure 3b).

Effect of contact time

The impact of the primary concentration of nickel and contact time on the removal of nickel by magnetite from aqueous was studied (Figure 3c). The effect of stir time was studied in the time range of 15-30 min. As shown in this Figure, the recovery of analyte increased in the first 20 min and then stayed almost constant after 20 min. As a result, stir time of 20 min was used as the optimum recovery time in this experiment.

Effect of ligand concentration

Dimethylglyoxime (DMG) was chosen as the chelating agent in the proposed method. Thus, the impact of the DMG amount of the Ni (II) recovery was studied in the range of 0 to2×10^{-4}molL^{-1} (Figure3d). The recovery of Ni (II) steadily increases with increasing DMG up to5×10^{-5}molL^{-1} with an important difference in sensitivity and then remains constant. Hence, 1×10^{-4} mol L^{-1} of DMG solution was selected as the optimum concentration for overcoming extractable interference in this experiment.

Selection of Eluent Parameters

A suitable eluent must have the full elution complete the absorbed analyte. In this research, according to the type of absorbent, four solutions, including acetonitrile:HNO_3 2%(v/v), methanol: HNO_3 2% (v/v), ethanol: HNO_3 2% (v/v), and water: HNO_3 2% (v/v) were compared(Fig. 3e). It was found that the analyte can be eluted quantitatively within the whole ethanol: HNO_3 2% (v/v) solution. Therefore, the ethanol: HNO_3 2% (v/v) solution was chosen as the eluent. The effect of eluent volume on the quantitative elution of analyte was tested by2-7 ml ethanol: HNO_3 2% (v/v) solution. It was observed that 3 ml ethanol: HNO_3 2% (v/v) solution was adequate to provide an acceptable adjustment for the analytes. In addition, the analytes' elution time was optimized by changing the time from 10 to 25 min. It can be concluded thatthe elution time has little effect on extraction recovery. As a result, 15 min was selected for the optimum elution time. Finally, 3 ml of ethanol: HNO_3 2% (v/v) solution with 15 min was used as the optimum sample.

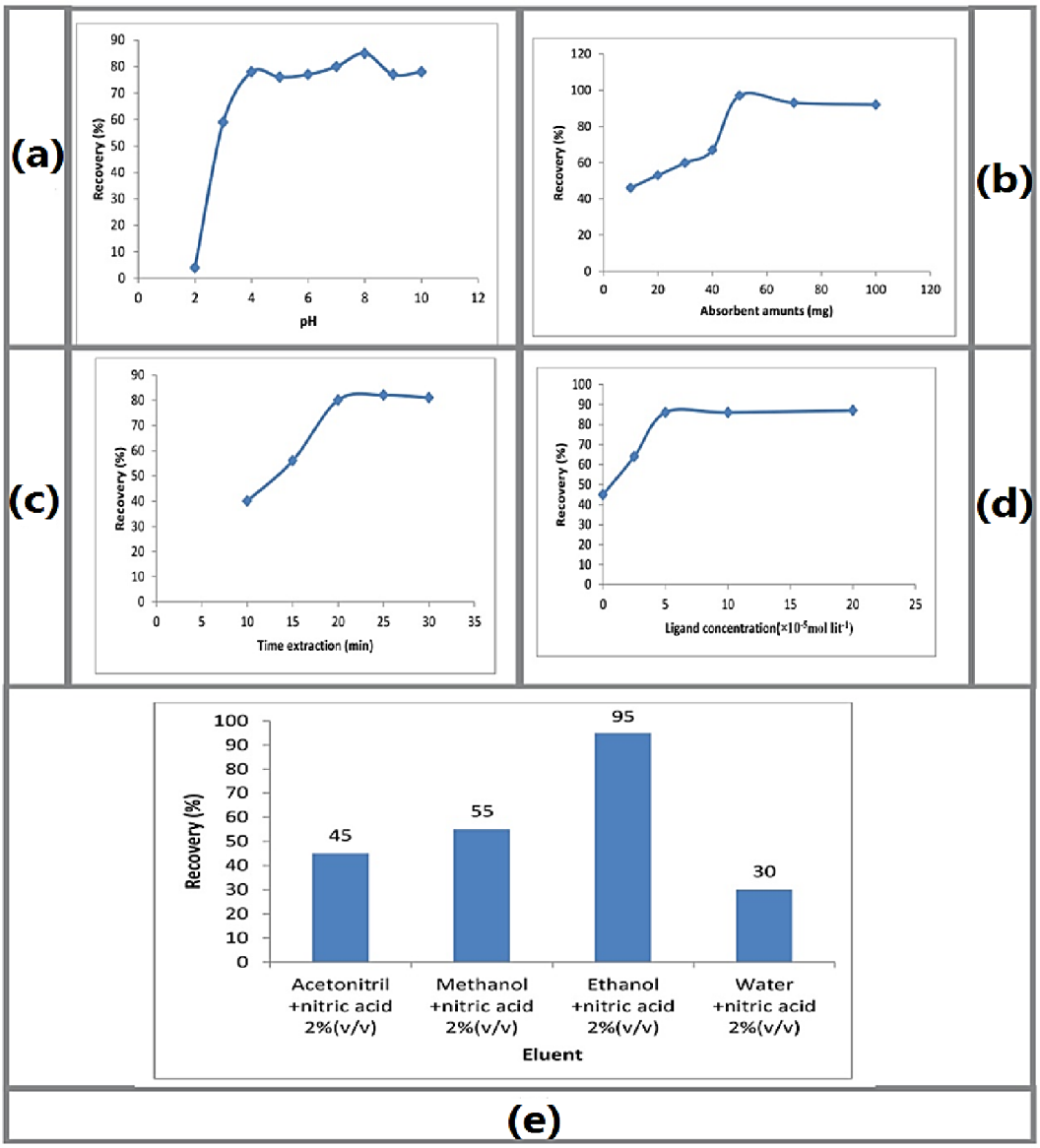

Figure 3. (a) Effect of pH on the adsorption of Nickel on Fe-[DABCO-PDA], (b) the amount of Fe-[DABCO-PDA] in extraction phase, (c) effect of adsorption contact time (min), (d) effect of ligand concentration on recovery of Nickel, and (e) effect of the type of the extraction solvents on the recovery nickel.

Effect of sample volume

The sample volume optimization was specified for calculating maximum applicable volumes and pre-concentration factor (PF) in DSPME. Hence, the impact of sample volume on the behavior of analytes retention was investigated using various sample volumes with the target ion being constant. The sample solutions containing 2 µg target ions were diluted in the range of 5 to 250 ml. The results showed that 100 ml is the highest sample volume that the quantitative extraction of analytes was obtained. For example, at volumes greater than 100 ml, the recovery of nickel decreased. For the elution volume of 3 ml, the optimum sample volume was selected as 100 ml. Therefore, the PF was obtained as 33.3 extraction samples for the analysis.

Extraction samples for analysis

A 25 ml sample solution containing nickel was placed in an Erlenmeyer. Next, 50 mgFe-[DABCO-PDA] NPs and 5×10^{-5}mol L^{-1} ligand DMG were added to the solution at a pH of 8. Next, the mixture of sample solution and sorbent was stirred for 20 min to help the dispersion of Fe-[DABCO-PDA] NPs in the sample solution. Following the extraction, a powerful magnet was spotted at the Erlenmeyer bottom for separating Fe-[DABCO-PDA] NPs from the aqueous solution. Afterward, the aqueous phase was dropped and Fe-[DABCO-PDA] NPs stayed in the Erlenmeyer. For desorbing the analyte, 3 ml of ethanol: HNO_3 2% (v/v) solution was added to Erlenmeyer containing Fe-[DABCO-PDA] NPs and stirred for 15 min. Ultimately, a powerful magnet was used for separating the sorbent in the organic phase of the stationary phase and the analyte in the solution was analyzed by FAAS.

Effect of matrix

The interference impact was a critical phase for verifying the selectivity of the suggested method. The effect of interference can be just explained by the extraction phase. The interfering of the cations, as well as anions with different concentrations added to the solution containing nickel and the limits of the tolerance, was determined for the interfering ions. The effects of cations on the recoveries of the analytes were investigated. The extraction process under the optimum conditions for nickel has a low interference effect and shows a high selectivity. The highest amount making change lower than 10% was defined as the tolerance limit of coexisting on in the recovery of the analytes. The findings indicated that 5 mg L^{-1} F^-, I^-, Cl^-, Br^-, NO_3^-, and CO_3^-, 5mg L^{-1} Na^+, K^+, Li^+,

Ca^{+}, Ba^{2+}, and Mg^{2+}, 0.01 mg L^{-1} Fe^{+3}, Cr^{+6}, and pb^{+2}, and 0.3 mgL^{-1} Cu^{+2}, Co^{+2}, and Mn^{+2} had no substantial efficacy on extraction and determination of the analyte.

The mechanism of the adsorption of nickel species by Fe-[DABCO-PDA] NPs

The present study was conducted to propose a mechanism that explains who adsorption is affected by coupling two or more mechanisms such as electrostatic interaction[52], ion exchange[53],physical adsorption[54], hard/soft acid-base interaction[55],and surface complexation[56]. In this regard, functional groups on the adsorbent surface with oxygen atoms have an important function in the nickel adsorption. The suggested mechanism in this reaction is the increase in the coordination number of Ni^{+2} in nickel bis(dimethylglyoximate) complex by the oxygen atom of Fe-[DABCO-PDA] NPs (Figure 4). This mechanism is in good agreement with the study of Geswat et al[57].

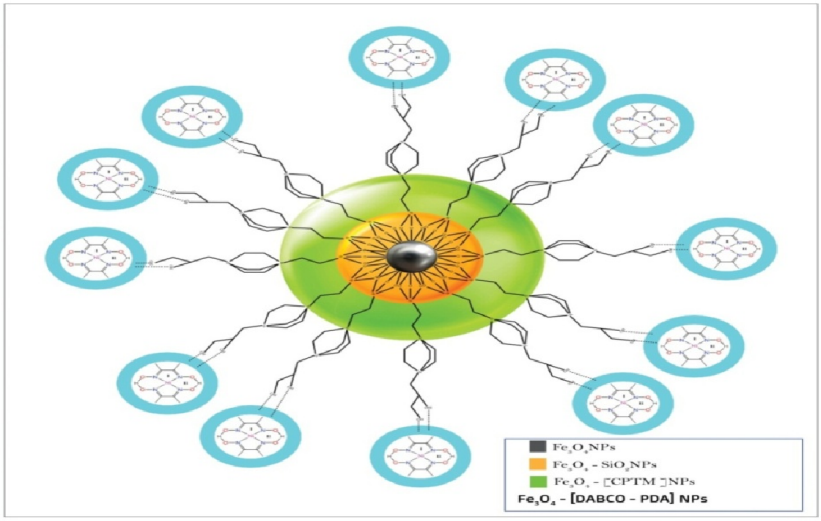

Figure 4. Schematic image related to the mechanism of nickel adsorption.

Analytical performance

The analytical parameters of the current study include linear dynamic ranges, the limit of detection (LOD), and limit of quantification (LOQ) of recovery, relative standard deviation (RSD%), precision, and pre-concentration factor (PF) of total results are shown in Table2. By applying this method on a chocolate base sample, the accuracy of this method was investigated on chocolate55%, 75%, and 85% samples and Shoniz chocolate. All samples were spiked with nickel and recovery values were examined. The results showed that the amount of nickel in chocolate samples was between 41.2 to 181.5 µg Kg^{-1}(Table3).The relative errors computed for the samples represented the great precision of this method. Moreover, the recovery values were highly satisfying in the 92-

97% range, validating the precision of the proposed approach. The results showed that by increasing the percentage of chocolate in the samples, the amount of nickel was increased.

Table 2. The analysis results of nickel in chocolate samples and addition /recovery for the application of the proposed method (n=5).

Sample	Real sample (µg Kg^{-1})		Added(µg Kg^{-1})	Founded(µg Kg^{-1})	Recovery(%)	RSD (%)
	Found	RSD (%)				
Chocolate 55%	41.2	4	50	89.9	97.4	2.7
Chocolate 75%	57	3.5	50	103.6	93.2	1.5
Chocolate 85%	90.2	1.8	50	138.8	97.2	2.7
Shoniz	181.5	7	50	231.2	99.4	2.9

Table 3. Analytical performance of the proposed method.

Parameters	Ni(II)
Linearity (µg Lit^{-1})	1-250
Limit of Detection (µg Kg^{-1})	0.18
Limit of Quantification (µg Kg^{-1})	0.6
Range of recovery(%)	92-97%
Precision (RSD %)	1.8-4%
Concentration factor (PF)	33.3
Sample volume (ml)	100

Moreover, the figure of merit of the proposed method is compared to other pre-concentration methods (Table4). It indicates that the suggested method is better than other methods in many parameters. Other advantages of this method include high speed, low-cost, sensitivity and selectivity of the adsorbent.

Table 4. Comparison of the preconcentration and determination of Ni.

Method	LOD (µg Kg^{-1})	RSD (%)	Recovery (%)	PF	Refs
UA-HF-LPME-FAAS	0.03	≤10	104.3	82	[58]
UA-CPE-FAAS	0.78	3.8	100.6	53.9	[59]
DLME-SFO-FAAS	1.27	3.21	95-100.5	27.1	[60]
DLME-FAAS	0.32	-	92.7	26	[61]

VA-IL-DLME-FAAS	0.3	2.5-3.6	96.5	75	[62]
SPE-FAAS	0.51	3.6	96.5	62.5	[63]
SPE-FAAS	0.25	2.1	103	25	[64]
SPE-FAAS	0.15	0.83-1.36	95	50	[65]
PV-IS-DLLE	0.1	4.8	98-114	17	[66]
DMSPE-FAAS	0.18	1.8-3.5	92-97	33.3	This work

UA-HF-LPME: Ultrasound assisted- hollow fiber- liquid phase microextraction; **UA-CPE:** Ultrasound assisted-Cloud point extraction; **DLME-SFO:** Dispersive liquid microextraction - solidification of floating organic droplet; **VA-IL-DLME:** vortex assisted - Ionic liquid-Dispersive liquid microextraction; **SPE:** Solid phase extraction; **PV-IS-DLLE**: Pressure variation-In syringe-Dispersive liquid liquid micro extraction; **DMSPE**, Dispersive micro Dispersive Solid phase extraction; **FAAS:** flame atomic absorption spectrometry.

Validation studies

A Validation test should be performed before using the proposed method to analyze chocolate samples. Two studies were performed to confirm this method. The first analysis was 85% chocolate samples containing Ni ions, which were performed by the standard laboratory of the Food and Drug Administration of Iran.A standard sample was prepared according to the method, which described "in 2.4 section". Then, the prepared sample was diluted in a ratio of 1:10 for two analytes in the linear range of the method.The proposed method was then applied to the prepared real samples.The results were in good agreement with the values reported in both analyses.Statistically, the t_{crit} values (df=2 at 95% confidence level) were higher than t_{exp} values.This indicates that there is no significant error in the results (Table5).

Table 5. Applications of the proposed coupled to the selected standard sample for validation of the method (n=3).

Sample	Reported values ($\mu g.kg^{-1}$) [a]	Measured ($\mu g.kg^{-1}$) [b]	RSD (%)	Recovery (%)	t_{exp} [c]
	Ni	Ni	Ni	Ni	Ni
Chocolate 85%	63	52.31 ± 1.12	3.45	98.62	3.38

a: After 10-fold dilution of the pre-treated standard sample where the reported values for Ni is 0.63 $mg.kg^{-1}$.
b: The mean value ± standard deviation based on three replicate determinations.
c: $t_{exp} = \frac{|\mu - \bar{x}|\sqrt{n}}{S}$, where t_{exp} was statistical value (for 2 degrees of freedom, the critical value of t at the 95% confidence level is 4.30), μ was the reported values, x was the experimental mean value, n was the number of independent determinations, and S was the standard deviation.

In another study, accuracy was determined by comparing nominal concentrations with the obtained concentrations. Accuracy was obtained by calculating the relative standard deviation (RSD) using repeatability (accuracy during the day) and reproducibility (accuracy between days) during 1 day

and on three different days. The experiments were performed at concentrations of 5, 30, and 70 µg Kg^{-1}. Acceptable recovery and reproducibility were obtained for all analytes in the recovery range (Table6).

Table 6. Intra-day and inter-day accuracy (as recovery%) and precision (as RSDs%) of the method for the chocolate sample (n=3).

Analyte	Intra-day, (Recovery ± RSD) %			Inter-day, (Recovery± RSD) %		
	5 µg.kg^{-1}	30 µg.kg^{-1}	70 µg.kg^{-1}	5 µg.kg^{-1}	30 µg.kg^{-1}	70 µg.kg^{-1}
Ni	97.3 ± 1.3	98.4 ± 1.6	101.3 ± 2.1	98.9 ± 3.2	99.8 ± 2.1	96.8 ± 3.1

Conclusions

In the present study, a new type of magnetic Fe-[DABCO-PDA] NPs was provided and utilized as a novel adsorbent in DMSPE for the nickel pre-concentration. Before FAAS determination, magnetic nanoparticles modified with ionic liquid Fe-[DABCO-PDA] NPs with (DMG) ligand were used for pre-concentration and extraction of nickel. The adsorption behaviors of the nickel on the Fe-[DABCO-PDA] NPs were studied. The pH of the solution, extraction time, adsorbent dosage, ligand concentration, mobile phase for the elution, and pre-concentration factor were considered as the optimum parameters. An external magnet was used for separating the magnetic sorbent in the aqueous step. The proposedmethod is fast, simple, effective, highly compatible with the presence of other ions, highly sensitive, with proper recovery, and eco-friendly. Therefore, it might be regarded as a great choice for determining nickel content in a chocolate sample.Also, this method can be studied to measure heavy metals in other samples such as milk and its products.

References

[1] B. Feist, R. Sitko, *Food Chem*.,249, 38 (2018).

[2] U. Villanueva, J. C. Raposo, J. M. Madariaga, *Microchem. J.,*106, 107 (2013).

[3] Ş. Saçmacı, M. Saçmacı, *Appl. Organomet. Chem*.,31, e4081 (2017).

[4] S. M. Sorouraddin, M. A. Farajzadeh, M. Ghorbani, *J. Iran. Chem. Soc.*,15, 201 (2018).

[5] M. Sadeghi, F. Shiri, D. Kordestani, P. Mohammadi, A. Alizadeh, *J. Iran. Chem. Soc.,*15, 753 (2018).

[6] N. B. Ivanenko, N. D. Solovyev, A. A. Ivanenko, A. A. Ganeev, *Arch Environ Contam Toxicol*.,63, 299 (2012).

[7] M. Güldaş, A. F. Dagdelen, G. F. Biricik, *J. Food Agric. Environ*., 56, 223 (2008).

[8] S. Saracoglu, K. O. Saygi, O. D. Uluozlu, M. Tuzen, M. Soylak, *Food Chem*.,105, 280 (2007).

[9] C. Ieggli, D. Bohrer, P. Do Nascimento, L. De Carvalho, *Food Chem*.,124, 1189 (2011).

[10] R. J. Cassella, D. M. Brum, N. F. Robaina, C. F. Lima, *Fuel*.,215, 592 (2018).

[11] S. M. Sorouraddin, S. Nouri, *Anal. Methods.*,8, 1396 (2016).

[12] Ş. M. Yolcu, M. Fırat, D. S. Chormey, Ç. Büyükpınar, F. Turak, S. Bakırdere, *Bull. Environ. Contam. Toxicol.*,100, 715 (2018).

[13] N. Khorshidi, A. Niazi, *Sep. Sci. Technol*.,51, 1675 (2016).

[14] F. Shemirani, S. M. Behgozin, *J. Iran. Chem. Soc*.,15, 1907 (2018).

[15] J. O. Vinhal, R. J. Cassella, *Spectrochim. Acta B*.,151, 33 (2019).

[16] L. A. Meira, J. S. Almeida, F. d. S. Dias, P. P. Pedra, A. L. C. Pereira, L. S. Teixeira, *Microchem. J*.,142, 144 (2018).

[17] R. R. Greenberg, P. Bode, E. A. D. N. Fernandes, *Spectrochim. Acta B*.,66, 193 (2011).

[18] J. Luo, F. Xu, J. Tu, X. Wu, X. Hou, *Microchem. J*.,132, 245 (2017).

[19] A. Jerše, R. Jaćimović, N. K. Maršić, M. Germ, H. Šircelj, V. Stibilj, *Microchem. J*.,137, 355 (2018).

[20] Z. Xuxu, L. Jianjie, G. Aiguo, W. Danhong, Z. Min, *At. Spectrosc.*,38, 77 (2017).

[21] S. Chen, J. Yan, J. Li, D. Lu, *Microchem. J*.,147, 232 (2019).

[22] N. R. Biata, K. M. Dimpe, J. Ramontja, N. Mketo, P. N. Nomngongo, *Microchem. J.*,137, 214 (2018).

[23] M. Krawczyk, M. Jeszka-Skowron, *Microchem. J.,*126, 296 (2016).

[24] S. Chen, S. Zhu, D. Lu, *Spectrochim. Acta B.*,139, 70 (2018).

[25] M. Krawczyk-Coda, *Spectrochim. Acta B*.,129, 21 (2017).

[26] M. M. Seitkalieva, V. V. Kachala, K. S. Egorova, V. P. Ananikov, *ACS Sustain. Chem. Eng.*,3, 357 (2014).

[27] H. Wang, H. Zhang, S. Wei, Q. Jia, *J. Chromatogr. A*.,1566, 23 (2018).

[28] A. K. Tripathi, Y. L. Verma, R. K. Singh, *J. Mater. Chem. A*.,3, 23809 (2015).

[29] G. Liu, P. Su, L. Yang, Y. Yang, *J. Sep. Sci.*,38, 3936 (2015).

[30] S. Chen, X. Qin, W. Gu, X. Zhu, *Talanta*.,161, 325 (2016).

[31] T. Liu, Y.-H. Lai, Y.-Q. Yu, D.-Z. Xu, *New J. Chem*.,42, 1046 (2018).

[32] F. Shirini, M. S. N. Langarudi, N. Daneshvar, M. Mashhadinezhad, N. Nabinia, *J. Mol. Liq*.,243, 302 (2017).

[33] N. Jamasbi, M. Irankhah-Khanghah, F. Shirini, H. Tajik, M. Langarudi, *New J. Chem*.,42, 9016 (2018).

[34] I. De la Calle, M. Menta, F. Séby, *Spectrochim.Acta B*.,125, 66 (2016).

[35] M. Llaver, E. A. Coronado, R. G. Wuilloud, *Spectrochim. Acta B*.,138, 23 (2017).

[36] B. Fahimirad, A. Asghari, M. Rajabi, *Microchimica Acta.*,184, 3027 (2017).

[37] Z. Es' haghi, G. R. Bardajee, S. Azimi, *Microchem. J*.,127, 170 (2016).

[38] N. Jalilian, H. Ebrahimzadeh, A. A. Asgharinezhad, *Microchem. J*.,143, 337 (2018).

[39] C. Magoda, P. N. Nomngongo, N. Mabuba, *Microchem. J.*,128, 242 (2016).

[40] M. Rajabi, A. G. Moghadam, B. Barfi, A. Asghari, *Microchimica Acta*.,183, 1449 (2016).

[41] A. L. Capriotti, C. Cavaliere, F. Ferraris, V. Gianotti, M. Laus, S. Piovesana, K. Sparnacci, R. Z. Chiozzi, A. Laganà, *Talanta*.,178, 274 (2018).

[42] W. Stöber, A. Fink, E. Bohn, *J. Colloid Interface Sci*.,26, 62 (1968).

[43] N. Fattahi, A. Ramazani, V. Kinzhybalo, Silicon.,11, 1745 (2019).

[44] A. Ying, Y. Ni, S. Xu, S. Liu, J. Yang, R. Li, *Ind. Eng. Chem. Res*.,53, 5678 (2014).

[45] K.-C. Kim, E.-K. Kim, J.-W. Lee, S.-L. Maeng, Y.-S. Kim, *CAP*.,8, 758 (2008).

[46] H. Yan, J. Zhang, C. You, Z. Song, B. Yu, Y. Shen, *Mater. Chem. Phys.*,113, 46 (2009).

[47] D. Xiao, C. Zhang, J. He, R. Zeng, R. Chen, H. He, *Sci. Rep*.,6, 38106 (2016).

[48] H. Sahebi, E. Konoz, A. Ezabadi, *New J. Chem*.,43, 13554 (2019).

[49] A. Ghorbani-Choghamarani, M. Norouzi, *J. Magn. Magn. Mater*.,401, 832 (2016).

[50] Y. Kishi, S. Shigemi, S. Doihara, M. Mostafa, K. Wase, *Hydrometallurgy.*,47, 325 (1998).

[51] F. Scholz, H. Kahlert, *Chem. Texts*.,1, 7 (2015).

[52] S. Dubey, S. Banerjee, S. N. Upadhyay, Y. C. Sharma, *J. Mol. Liq*.,240, 656 (2017).

[53] A. Z. M. Badruddoza, Z. B. Z. Shawon, M. T. Rahman, K. W. Hao, K. Hidajat, M. S. Uddin, *Chem. Eng. J.,*225, 607 (2013).

[54] N. N. Nassar, *J. Hazard. Mater*.,184, 538 (2010).

[55] D. Vollath, W.-V. V. G. KGaA, *Management*.,7, 865 (2008).

[56] M. Xu, H. Wang, D. Lei, D. Qu, Y. Zhai, Y. Wang, *J. Env.S*.,25, 479 (2013).

[57] A. Osunlaja, N. Ndahi, *J. Ameh,Afr. J. Biotechnol*.,8 (2009).

[58] K.C. Hsu, C.F. Lee, Y.Y. Chao, C.C. Hung, P.C. Chen, C.H. Chiang, Y.L. Huang.,*J. Anal. At. Spectrom.,*31, 2338 (2016).

[59] N. K. Temel, K. Sertakan, R. Gürkan, *Biol. Trace Elem. Res.*,186, 597 (2018).

[60] Y. Wang, J. Zhang, B. Zhao, X. Du, J. Ma, J. Li, *Biol. Trace Elem. Res.*,144, 1381 (2011).

[61] R. Khani, F. Shemirani, *Food Anal. Method*.,6, 386 (2013).

[62] N. Altunay, A. Elik, R. Gürkan, *Microchem. J*.,147, 277 (2019).

[63] Y. K. Wang, S. T. Gao, J. J. Ma, J. C. Li, *J. Chin. Chem. Soc*.,59, 1468 (2012).

[64] M. R. Pourjavid, M. Arabieh, S. R. Yousefi, M. R. Jamali, M. Rezaee, M. H. Hosseini, A.

A. Sehat, *Mater. Sci. Eng. C.*,47, 114 (2015).

[65] S. Khazaeli, N. Nezamabadi, M. Rabani, H. A. Panahi, *Microchem. J.*,106, 147 (2013).

[66] J. A. Barreto, R. d. S. de Assis, R. J. Cassella, V. A. Lemos, *Talanta.*,193, 23 (2019).